International Journal of Applied Mathematics
Volume 38 No. 12s, 2025
ISSN: 1311-1728 (printed version); ISSN: 1314-8060 (on-line version)

PEMFC PARAMETER ESTIMATION FOR RENEWABLE ENERGY APPLICATIONS USING STARFISH OPTIMIZATION

Fadhel A. Jumaa[1], Nabeel alhasan[2], Ghaith M. Fadhil[3]*

[1] Department of Electrical Engineering, Technical Institute, Al-Furat Al-Awsat Technical University, Kufa, Najaf, 54001, Iraq, dr-fadhela.jumaa@atu.edu.iq.

[2] Department of Electrical Engineering, Technical Institute, Al Furat Alawsat Technical University, Kufa, Najaf, 54001, Iraq, nabeel.talib@atu.edu.iq.

[3] Civil Engineering Department, College of Engineering, Al-Qasim Green University, Babylon 51013, Iraq, Kaithmajed@wrec.uoqasim.edu.iq.

Abstract

This research develops and evaluates the Starfish Optimization Algorithm (SFOA) for finding the best parameters of a Proton Exchange Membrane Fuel Cell (PEMFC). The SFOA is a metaheuristic optimization algorithm, which is applied for accurate estimating the model parameters for the minimization of the error between the experimental and calculated values. The performance of SFOA algorithm was tested on four different types of commercial fuel cells: 250W PEMFC, BCS-500 PEMFC, AVISTA SR-12 PEMFC and Temasek 1kW PEMFC, under various operating conditions, including varying temperature and reactant gas pressures, to ensure the reliability of the proposed models in different operating environments. The results showed that the performance of the SFOA algorithm varied depending on the cell type. SFOA algorithm achieved: 0.000607079 RMSE and Efficiency: 99.96166766% for the 250 W PEMFC; 0.000291RMSE and 98.5639177% Efficiency for BCS-500 W PEMFC; 0.00510784 RMSE and 99.8043958% Efficiency for AVISTA SR-12 (500 W) PEMFC; and 0.00094235 RMSE and 99.8989187% Efficiency for Temasek 1 kW PEMFC. Results demonstrate the ability of the SFOA algorithm to have a good balance between search accuracy and convergence speed. This study confirms that the nature-inspired optimization algorithms are an effective and accurate tool in estimating PEMFC fuel cell parameters, contributing to improved mathematical models and the development of more efficient control systems for various clean energy applications.

Keywords: 250W PEMFC, AVISTA SR-12, BCS-500, SFOA, and Temasek 1kW.

Introduction

Energy underpins development, yet despite rising demand, fossil fuels still supply 80–90% of global needs, driving global warming, sea-level rise, and pollution [1]. Accelerating the transition to clean energy is therefore imperative for environmental, health, and economic sustainability. Hydrogen fuel cells provide high efficiency with zero local emissions and proton exchange membrane fuel cells (PEMFCs) in particular have high potential in transport and distributed generation applications, and portable uses due to low temperature, fast start-up, and typical efficiencies of 40–50% [2, 3]. PEMFCs' performance is hard to optimize because the

Received: August 14, 2025

ISSN: 1311-1728 (printed version); ISSN: 1314-8060 (on-line version)
cells are nonlinear and depend on hard-to-measure physical/electrochemical parameters (e.g., membrane resistance, ionic transport, electrode-loss coefficients) [4, 5]. Accurate parameter estimation is thus crucial for faithful models used in design, control, and performance prediction. Classical numerical methods often falter on these nonlinear couplings, motivating nature-inspired metaheuristics that better explore the search space and avoid local minima. Yet their effectiveness varies with convergence behavior and exploration–exploitation balance, necessitating careful evaluation to identify the most suitable algorithms for fuel-cell applications [6, 7].

PEMFC modeling follows two paths: mechanistic models that resolve transport and electrochemistry, and semi-empirical models that map operating variables to the voltage–current (V–I) curve; the latter dominate practice for speed but rely on accurately estimating indirect parameters, making estimation the core bottleneck. Because PEMFC behavior is multivariable and nonlinear, classical numerical methods often falter on nonconvex error surfaces, motivating nature-inspired metaheuristics for parameter extraction. Recent studies report gains using Improved Manta Ray Foraging Optimization (IMRFO) with sine–cosine boosting [8], Quantum-coded Pathfinder Algorithm (QPFA) [9], Chaotic Mayfly Algorithm (CMA) [10], Bald Eagle Search (BES) outperforming Gravitational Search Algorithm (GSA)/Differential Evolution (DE) [11], and further advances from Improved Salp Swarm Algorithm (ISSA) [12], Improved Teamwork Optimizer [13], Gorilla Troops Optimizer (GTO) [14], Moth-Flame Optimization (MFO) [15], Cuckoo Search (CS) [16], War Strategy Optimization (WSO) [1], Lévy Chaotic Artificial Hummingbird Algorithm (LCAHA) [17], Artemisinin Optimization (AO) [18], Atomic Orbital Search (AOS) [19], and Modified/Enhanced Farmland Fertility Algorithm (MFFA) [20]. Yet common issues persist susceptibility to local minima, slow or unstable convergence, and hyperparameter sensitivity consistent with the No-Free-Lunch Theorem (NFLT) that no single optimizer dominates across problems [21, 22]. These gaps, compounded by variation across PEMFC types and operating regimes, underscore the need for methods that balance exploration vs. exploitation, converge stably, and generalize across conditions. In response, our methodology concentrates on the SFOA and rigorously validates it on real V–I datasets with transparent protocols (metrics, seeds, and statistical tests), aiming for reliable, high-fidelity PEMFC parameter identification [23].

This work focuses exclusively on the SFOA algorithm [24] for PEMFC parameter estimation, evaluating it on four stacks (250 W, BCS-500 W, AVISTA SR-12, Temasek 1 kW) across varied temperatures and gas pressures with 30 independent runs per case. We (i) formulate a physically bounded SFOA-based estimator for the semi-empirical model, (ii) adopt a transparent evaluation protocol reporting MAE/RMSE and runtime as mean ± SD, (iii) demonstrate fast, stable convergence and high estimation accuracy across all operating regimes, (iv) analyze hyperparameter sensitivity (population size, iterations) and recommend practical defaults, (v) validate generalization via temperature/pressure variations with close agreement to measured V–I curves, (vi) benchmark against published baselines to show competitive or superior accuracy and stability, and (vii) document seeds/configurations to ensure reproducibility and facilitate adoption in PEMFC design and control.

International Journal of Applied Mathematics
Volume 38 No. 12s, 2025
ISSN: 1311-1728 (printed version); ISSN: 1314-8060 (on-line version)

1. Methods

1.1. Mathematical Modelling of PEMFC

A. PEMFC Background

PEMFC is a process that directly converts chemical energy contained in hydrogen into electrical energy by using hydrogen (H2) as fuel and oxygen (O2) as oxidant [25, 26]. Figure 1. gives a schematic representation of a typical configuration of a PEMFC. At the anode, pressurized hydrogen is fed as the main reactant by which the electrochemical conversion process takes place. Although the current system uses pure hydrogen, various mixtures of gases can be used, if the hydrogen concentration in the gas mixture is accurately determined. The hydrogen diffuses through the anode and makes it to the catalytic layer where the oxidation reaction can take place, producing protons and electrons according to [26].

At the cathode, oxygen is supplied to the cell, taken either from ambient air or a stream of pure oxygen. The oxygen molecules diffuse through the porous electrode in the direction of the catalytic layer, where they are reacted with the protons and electrons to produce water [27]. The end result of the overall electrochemical process in the fuel cell is electrical energy, with heat and liquid water as secondary products, with the latter condensing on the surface of the cathode catalyst particles. Precise control of these electrochemical reactions, and the control of heat and water transport phenomena in the cell, are important requirements for high-performance operation and long-life characteristics of the fuel cell system.

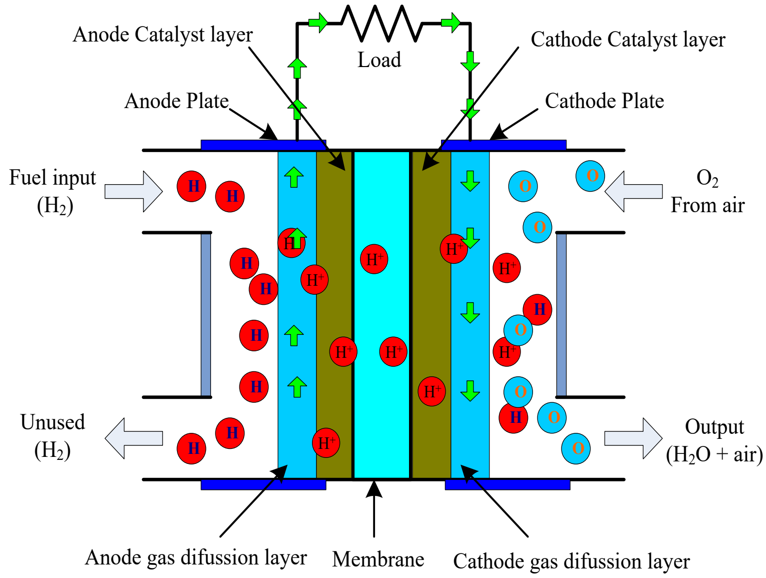

Fig. 1. Schematic diagram of PEMFC

B. PEMFC Stack Mathematical Model

The complete mathematical framework that describes the performance of a PEMFC fuel cell under various operating conditions is discussed in this section. The precision of the model depends on the correct extraction of seven parameters $\xi_1, \xi_2, \xi_3, \xi_4, \lambda, b, and\ R_C$. Due to the nonlinear and complex nature of the relationships between the variables, the use of traditional estimation methods often leads to inaccurate local solutions. Therefore, this research proposes novel SFOA algorithm that combine global and local search capabilities to achieve an effective

Received: August 14, 2025

International Journal of Applied Mathematics
Volume 38 No. 12s, 2025
ISSN: 1311-1728 (printed version); ISSN: 1314-8060 (on-line version)
balance between exploration and exploitation, thereby improving the accuracy of PEMFC model parameter identification.

The mathematical modeling of the PEMFC equivalent electrical circuit shown in Fig. 2 describe the interrelation between voltage, current, and electrical losses associated with internal electrochemical processes [5, 25, 28]. The output potential generated by an individual fuel cell can be determined using Equation (1).

$$V_{fc} = E_{nerst} - \Delta V_{act} - \Delta V_{ohm} - \Delta V_{con} \quad (1)$$

where E_{nerst} denotes reverse potential. ΔV_{act} is the loss due to activation loss caused by slow electrochemical reactions on the catalytic surfaces. ΔV_{ohm} is the ohmic loss resulting from the resistance of electrons at electrodes also the resistance of protons within the membrane. ΔV_{con} denotes concentration overpotential loss due to low gas concentrations at high currents. The overall voltage of a PEMFC stack comprising multiple cells connected in series can be calculated using $V_{stack} = N_{cells} \times V_{fc}$ where N_{cells} indicates the total number of cells in the stack.

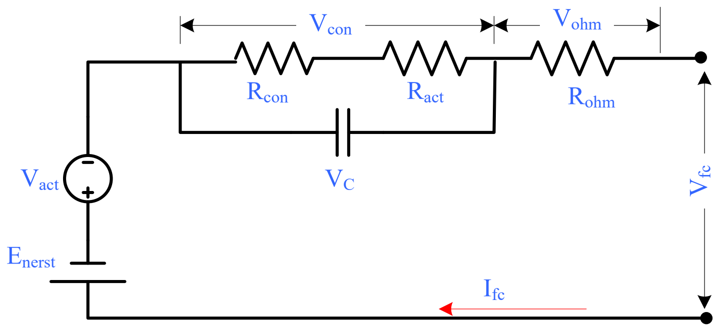

Fig 2. Electrical Equivalent circuit of PEMFC.

The reverse potential is estimated using the Nernst equation, which describes the relationship between the theoretical potential of the FC and key operational parameters such as temperature and pressure of the reacting gases:

$$E_{nerst} = 1.229 - (8.5 \times 10^{-4})\left(T_{fc} - 298.15\right) + 4.3085 \times 10^{-5} \times T_{fc} \times \left[\ln\left(P_{H_2}\right) + \ln\left(\sqrt{P_{O_2}}\right)\right] \quad (2)$$

where T_{fc} implies the absolute operating temperature (Kelvin). P_{H_2} denotes partial pressure of hydrogen gas. P_{O_2} denotes partial pressure of oxygen gas.

When using pure hydrogen and oxygen, the partial pressure of oxygen is given as reported in [29]:

$$P_{O_2} = RH_c \times P_{H_2O}^{sat} \left[\left(exp\left(\frac{4.192 \times \left(\frac{I_{fc}}{A}\right)}{T_{fc}^{1.334}} \right) \times \frac{RH_c \times P_{H_2O}^{sat}}{P_c} \right)^{-1} - 1 \right] \quad (3)$$

The partial pressure of hydrogen is estimated from the following equation:

Volume 38 No. 12s, 2025
ISSN: 1311-1728 (printed version); ISSN: 1314-8060 (on-line version)

$$P_{H_2} = 0.5 \times RH_a \times P_{H_2O}^{sat} \left[\left(exp\left(\frac{1.635 \times \left(\frac{I_{fc}}{A}\right)}{T_{fc}^{1.334}} \right) \times \frac{RH_a \times P_{H_2O}^{sat}}{P_a} \right)^{-1} - 1 \right] \quad (4)$$

where P_a and P_c denote inlet pressures at inlet channels of the FC stack (atm). RH_a and RH_c signify the relative humidity at the electrodes. $P_{H_2O}^{sat}$ is the vapor pressure of generated water at saturation, calculated from the relationship [30]:

$$\ln\left(P_{H_2O}^{sat}\right) = 2.95 \times 10^{-2}\left(T_{fc} - 273.15\right) - 9.18 \times 10^{-5} \times \left(T_{fc} - 273.15\right)^2 + 1.44 \times 10^{-7}\left(T_{fc} - 273.15\right)^3 - 2.18 \quad (5)$$

The activation losses is expressed by the formula [25]:

$$\Delta V_{act} = -\left[\xi_1 + \xi_2 \times T_{fc} + \xi_3 \times T_{fc} \times \ln\left(C_{O_2}\right) + \xi_4 \times T_{fc} \times \ln\left(I_{fc}\right)\right] \quad (6)$$

Where $\xi_1, \xi_2, \xi_3, and\ \xi_4$ denote experimental parameters. C_{O_2} is Oxygen concentration at the cathode electrode, calculated usings:

$$C_{O_2} = \frac{P_{O_2}}{5.08 \times 10^6} \times exp\left(\frac{498}{T_{fc}}\right) \quad (7)$$

The value of ΔV_{act} increases with decreasing oxygen concentration or at higher currents, due to the increased difficulty of electrochemical reactions around the cathode surface.

The Ohmic Loss, calculated using:

$$\Delta V_{ohm} = I_{fc} \times (R_M + R_C) \quad (8)$$

where R_M represents resistance of the membrane layer, and R_C implies the resistance due to motion of protons via the membrane. R_M is estimated using $R_M = (\rho_M \times l)/A$ where ρ_M presents specific resistance of the material, from which the membrane is produced (Ω·cm), l denotes thickness of membrane layer (cm), A is the membrane area. ρ_M is estimated from the following empirical relationship [31]:

$$\rho_M = \frac{181.6 \times \left[1 + 0.03\left(\frac{I_{fc}}{A}\right) + 0.062 \times \left(\frac{T_{fc}}{303}\right)^2 \times \left(\frac{I_{fc}}{A}\right)^{2.5}\right]}{\left[\lambda - 0.634 - 3 \times \left(\frac{I_{fc}}{A}\right)\right] \times exp\left[4.18\left(\frac{T_{fc} - 303}{T_{fc}}\right)\right]} \quad (9)$$

where λ is an adjustable parameter associated with membrane production.

The concentration Loss is calculated using:

$$\Delta V_{con} = -b \times \ln\left(1 - \frac{J}{J_{max}}\right) = -b \times \ln\left(1 - \frac{I_{fc}/_A}{J_{max}}\right) \quad (10)$$

where b denotes empirical constant that depends on the properties of the membrane and gases. J is the current density (A/cm²). J_{max} is the maximum possible current density before the concentration begins to drop sharply. As J approaches J_{max}, losses increase significantly due to the reduced mass transport efficiency of the gases.

International Journal of Applied Mathematics
Volume 38 No. 12s, 2025
ISSN: 1311-1728 (printed version); ISSN: 1314-8060 (on-line version)

C. Objective Function

The objective function is formulated as:

$$OF = min\,TSD\,(x) = min\sum_{i=1}^{N}\left(V_{exp}(i) - V_{est}(i)\right)^2 \quad (11)$$

where $V_{exp}(i)$ is the experimentally measured voltage at point i, $V_{est}(i)$ is the potential calculated from the mathematical model at the same point, N is the number of data points, and $x = [\xi_1\ \xi_2\ \xi_3\ \xi_4\ \lambda\ b\ R_C]$ represents the set of variables to be estimated.

The objectives are to reduce the error between the actually measured and numerically calculated voltage values at various current values. The model is subject to a set of operational constraints (Boundaries) that ensure that the values remain within the physical and reasonable limits for each parameter as provided in equation (17), the maximum and minimum limits of unknown parameters are changed like in Table 1.

$$\xi_{i,min} \le \xi_i \le \xi_{i,max},\ \ i = 1,2,3,4 \quad (12)$$

$$\lambda_{min} \le \lambda_i \le \lambda_{max} \quad (13)$$

$$b_{min} \le b_i \le b_{max} \quad (14)$$

$$R_{Cmin} \le R_C \le R_{Cmax} \quad (15)$$

Table 1. Upper and lower bounds of the optimized parameters.

Parameter	Lower Bound	Upper Bound
ξ_1	-0.8532	-1.1997
ξ_2	1.0×10^{-3}	5.0×10^{-3}
ξ_3	3.6×10^{-5}	9.8×10^{-5}
ξ_4	-2.6×10^{-4}	-0.954×10^{-4}
λ	10	23
b	0.0136	0.5
R_C	1.0×10^{-4}	8.0×10^{-4}

1.2. Starfish Optimization Algorithm (SFOA)

The SFOA is used here to tune PEMFC model hyperparameters by efficiently searching complex, high-dimensional spaces and selecting near-optimal parameter sets that improve accuracy [24]. Inspired by starfish feeding, locomotion, and regeneration, SFOA maintains a strong exploration (exploitation balance) less prone to local minima than gradient-based methods and more adaptive than purely random search. Its hybrid search adapts to problem size: a five-arm, five-dimensional exploration when the decision dimension L>5 enables broad coverage, while a one-dimensional intensified search for L≤5L accelerates convergence. This adaptivity typically achieves higher precision with fewer iterations and reduced runtime, making SFOA well-suited for the nonlinear, coupled parameter landscapes of PEMFC models

Volume 38 No. 12s, 2025
ISSN: 1311-1728 (printed version); ISSN: 1314-8060 (on-line version)
[24]. The SFOA approach includes three main stages: (1) Initialization phase, At the beginning of the algorithm, starfish positions are randomly generated within a predefined design area, expressed as a location matrix X, where N denotes the size of population and L denotes the dimension of the optimization problem. Initial locations are calculated using the equation:

$$X = \begin{bmatrix} x_{11} & x_{12} & \cdots & x_{1L} \\ x_{21} & x_{22} & \cdots & x_{2L} \\ x_{31} & x_{32} & \cdots & x_{3L} \\ \vdots & \vdots & \ddots & \vdots \\ x_{N1} & x_{N2} & \cdots & x_{NL} \end{bmatrix} \tag{16}$$

$$x_{ij} = lower_j + random\left(upper_j - lower_j\right), i = 1, 2, \ldots\ldots, N, \; j = 1, 2, \ldots\ldots, L \tag{17}$$

The fitness value of all candidates is then evaluated based on the objective function, allowing for an adaptive search mechanism. (2) Exploration Phase, the algorithm uses different tactics depending on the dimensionality of the optimization issue: For $L > 5$, a five-dimensional search is applied to optimize the large scale, for $L \leq 5$, a one-dimensional search is used to optimize the local optimization. The position update rule in the exploration phase is presented in Equation (20), where sine and cosine functions are used with parameters a and θ defined in Equation (21). If the modified location is outside the model parameters, the arms remain in their previous location. If $L \leq 5$, the location is upgraded using a one-dimensional search design according to Equation (22), where the starfish uses location information from other candidates to move one of its arms toward the nutrition source. (3) Exploitation phase, this phase consists of hunting and regeneration tactics. The starfish's location is updated based on the best location found, and the direction vectors d_n are calculated as in Equation (24), where $n = 1, 2, \ldots, 5$, which reflects the radial structure of the starfish and allows for accurate convergence towards the optimal solution. The flowchart of the SFOA is presented in Fig. 3.

$$X_{i,p}^{t+1} = \begin{cases} X_{i,p}^{t} + a\left(X_{best,p}^{t} - X_{i,p}^{t}\right)\cos\theta \,, & if\ rn \leq 0.5, \\ X_{i,p}^{t} + a\left(X_{best,p}^{t} - X_{i,p}^{t}\right)\sin\theta \,, & if\ rn > 0.5 \end{cases} \tag{18}$$

$$a = (2r - 1)\pi, \qquad \theta = \frac{\pi}{2} \cdot \frac{t}{t_{max}} \tag{19}$$

$$X_{i,p}^{t+1} = E_t X_{i,p}^{t} + a_1\left(\left(X_{k1,p}^{t} - X_{i,p}^{t}\right)\right) + a_2\left(\left(X_{k2,p}^{t} - X_{i,p}^{t}\right)\right) \tag{20}$$

$$E_t = \frac{t_{max} - t}{t_{max}} \cos\theta \,, \tag{21}$$

$$d_n = X_{best}^{t} - X_{np}^{t}, \qquad n = 1, 2, \ldots, 5 \tag{24}$$

Received: August 14, 2025

International Journal of Applied Mathematics
Volume 38 No. 12s, 2025
ISSN: 1311-1728 (printed version); ISSN: 1314-8060 (on-line version)

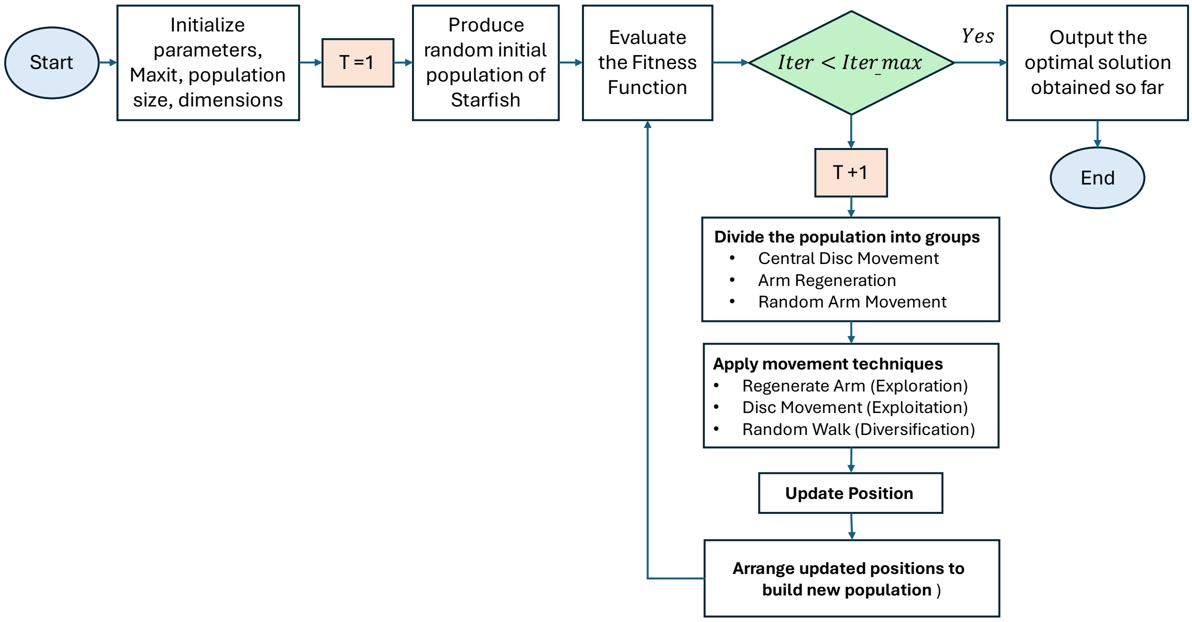

Fig. 3. Flowchart of the SFOA operation.

2. Results and Discussion

For result analysis, we apply the SFOA to identify the unknown parameters of four real PEMFC stacks (250 W, BCS-500 W, AVISTA SR-12 (500 W), and Temasek 1 kW) using measured voltage–current (I–V) data [5, 12, 32–34]. Each case is run 30 independent times (to ensure statistical reliability) with 200 maximum iterations and 30 search agents per run. The best parameter set from each run is chosen by the lowest objective-function (OF) value, and all searches respect physically realistic upper/lower bounds for every parameter. We report accuracy and stability via MAE, RMSE, SD, and summarize hardware-independent computational efficiency. Stack specifications are listed in Table 2, and SFOA's outcomes are benchmarked against published state-of-the-art methods (ASO, HHO, JAYA, FOA, ICA, SSO, GWO, SSA) to contextualize performance [27, 35–38, 12].

Table 2. Parameters of all PEMFCs tested in the study.

PEMFC	N_{Cells}	A (cm2)	L (μm)	$J_{Max}(mA/cm^2)$	$PH_2(atm)$	$P0_2(atm)$	T (K)
250 W PEMFC	24	27	127	860	1	1	343.15
BCS 500 W FC	32	64	178	469	1	0.2095	333
SR-12 500 W PEM	48	62.5	25	672	1.4763	0.2095	323

Temasek 1 kW stack	20	150	51	1500	0.5	0.5	323

2.1. Standard 250W PEMFC

The statistical analysis in Tables 3-4 proves that SFOA is efficient in the extraction of parameters of the 250-W PEMFC model with high accuracy and stability. It reached the minimum value of the objective function (0.642014) and the absolute SD (5.64x10^-4) of 30 independent runs, which showed a tight convergence. Correspondingly, MAE and RMSE are minimized compared with published baselines, which indicates that SFOA has an effective exploration-exploitation balance in the search space. The SFOA convergence plots seen in Fig 4 indicate a fast drop-in fitness at the very beginning, followed by fast stabilization, and the iteration-to-iteration rate of change confirms that the refinement is steady and without oscillation. The polarization analyses presented in Fig. 5, Fig. 6, and Fig. 7 further confirm the validity of the fitted model: simulated and measured I - V data agree well under different operating conditions. As expected, by increasing the temperature, cell voltage is increased at a given current density (enhanced kinetics), and by decreasing partial pressures of H2/O2, voltage is decreased due to limited diffusion. Collectively, these results confirm SFOA to be a robust, precise also computationally stable estimator for PEMFC parameter identification over operating regimes.

Table 3. Statistical study based on the final values of convergence curves for 250W PEMFC.

Result	SFOA
Min	0.642014492
Max	0.645005426
Mean	0.642261163
SD	0.000564189
MAE	0.000246671
RMSE	0.000607079
Efficiency	99.96166766

Table 4. Optimization results for 250W PEMFC based on the proposed methods and literature.

Parameter	ASO [35]	HHO [35]	JAYA [36]	SFOA
ξ_1	−1.109267	−1.10972	−0.9520	-1.156688
$\xi_2 \times 10^{-3}$	3.11831	3.4586	3.1	2.99848
$\xi_3 \times 10^{-5}$	6.176176	8.31679	8.0	3.60232
$\xi_4 \times 10^{-4}$	−1.419328	−1.51684	−1.9000	-1.55908
λ	17.65681	22.9454	23	23

Volume 38 No. 12s, 2025
ISSN: 1311-1728 (printed version); ISSN: 1314-8060 (on-line version)

b	0.053566	0.054264	0.0327	0.0545476
$R_C \times 10^{-4}$	1.00	3.83084	1.00	1.00
TSD	0.75884	0.64577	9.901	**0.642014**

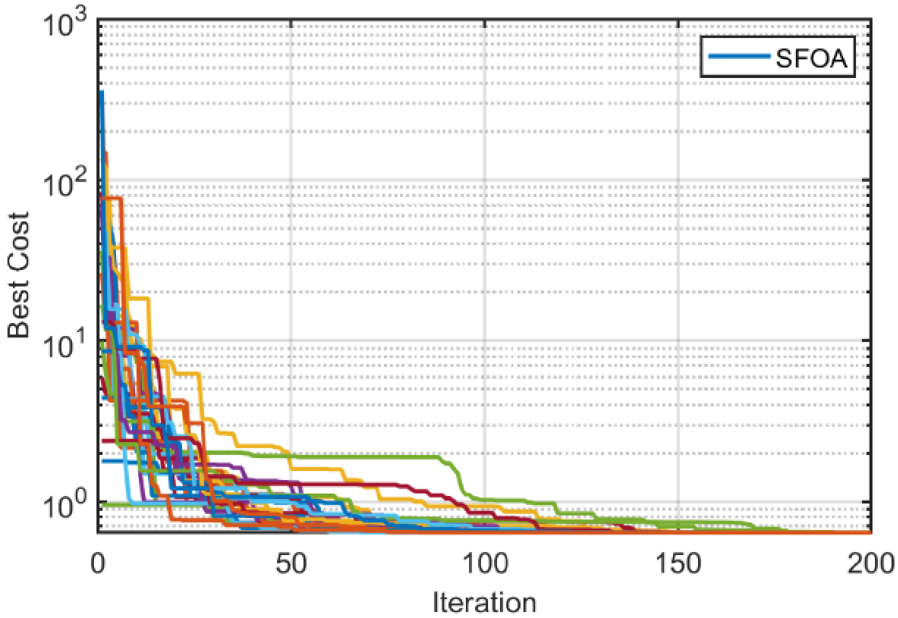

Fig. 4. Convergence curves for 30 runs for 250W PEMFC with SFOA algorithm

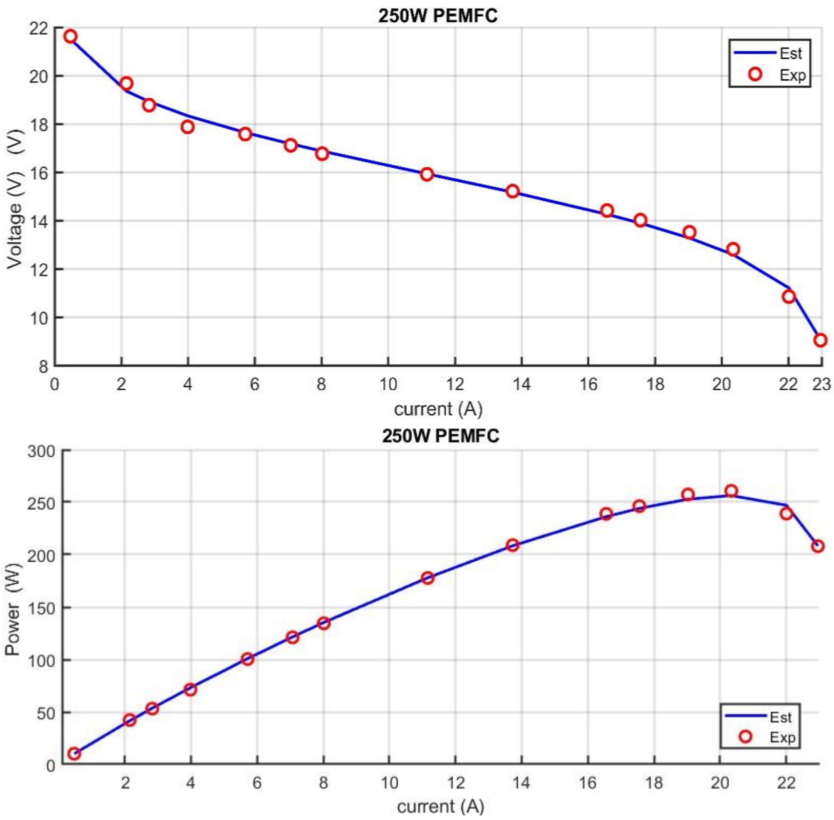

Fig. 5. Polarization curves of 250W PEMFC

Received: August 14, 2025

International Journal of Applied Mathematics
Volume 38 No. 12s, 2025
ISSN: 1311-1728 (printed version); ISSN: 1314-8060 (on-line version)

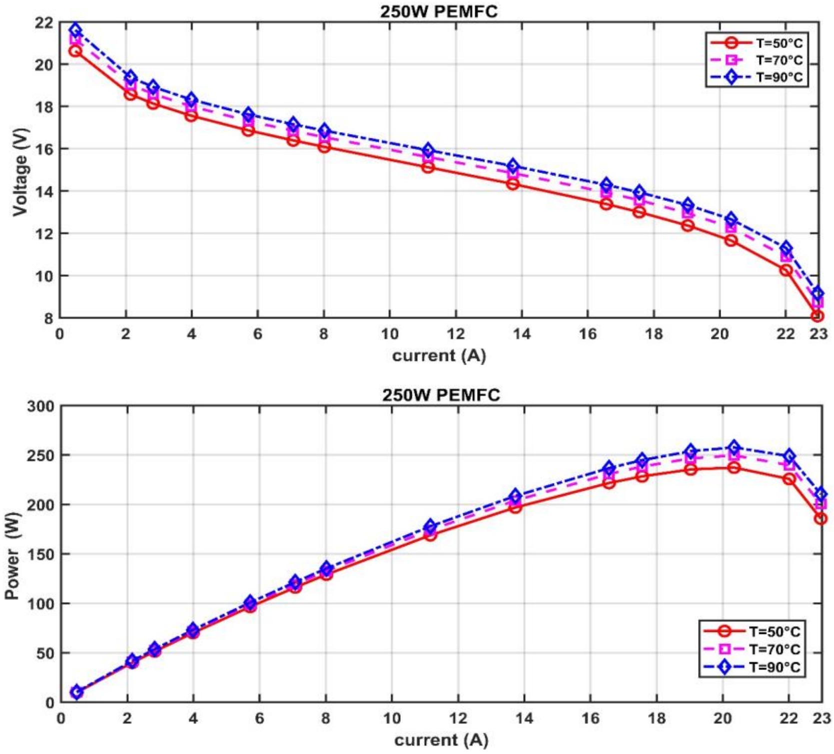

Fig. 6. Polarization curves of 250W PEMFC under temperature variation.

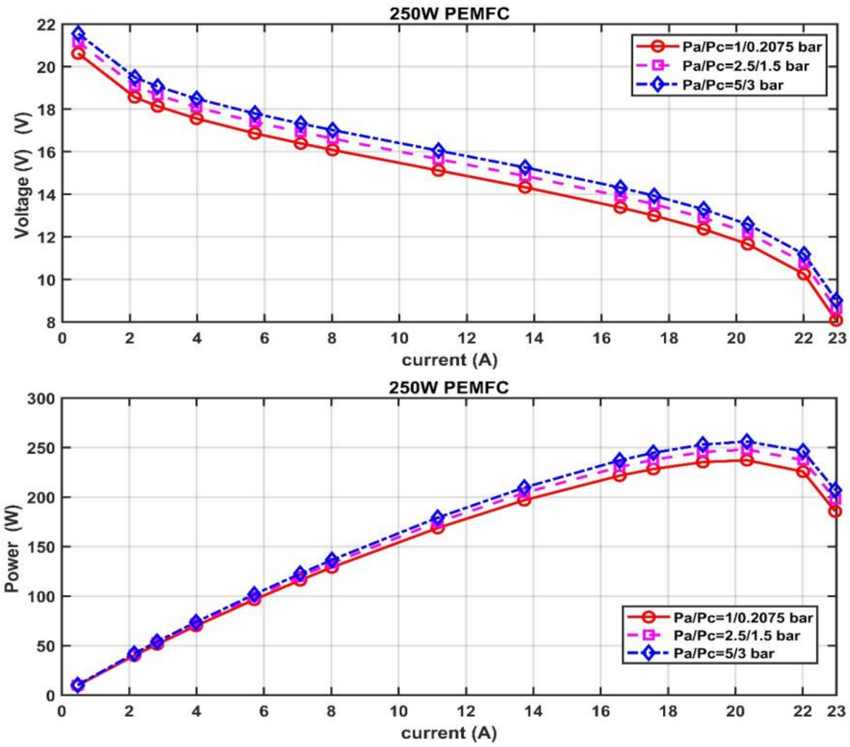

Fig. 7. Polarization curves of 250W PEMFC under gases pressure variation.

2.2. BCS 500W PEMFC

International Journal of Applied Mathematics
Volume 38 No. 12s, 2025
ISSN: 1311-1728 (printed version); ISSN: 1314-8060 (on-line version)
This section analyzes SFOA on the BCS-500 W PEMFC and shows it reliably identifies the model's unmeasured parameters and outperforms conventional baselines. The SFOA convergence curves shown in Fig. 8, Quantitatively, Table 5 reports SD = 0.00023797 and efficiency = 98.56%, confirming strong accuracy–stability trade-offs, while Table 6 shows TSD = 0.01158, improving upon conventional methods (e.g., FOA, ICA, SSO). Polarization-curve validation (Fig. 9) demonstrates a near one-to-one match between simulated and experimental I–V points, and stress tests under varying temperature and gas pressures (Fig. 10; and Fig. 11) show robust predictions across operating regimes. Overall, SFOA delivers high precision, low variance, and consistent convergence for the BCS-500 W stack, supporting accurate PEMFC modeling and dependable performance forecasting.

Table 5. Statistical study based on final values of convergence curves for BCS 500W PEMFC.

Result	SFOA
Min	0.01157837
Max	0.01289196
Mean	0.0117514
SD	0.00023797
MAE	0.00017303
RMSE	0.000291
Efficiency	98.5639177

Table 6. Optimization results for BCS 500W PEMFC based on the proposed methods and literature.

	FOA [27]	ICA [27]	SSO [37]	SFOA
ξ_1	-0.99282	-0.90864	−1.018	-0.87405
$\xi_2 \times 10^{-3}$	2.62	2.4798	2.3151	0.003087
$\xi_3 \times 10^{-5}$	3.746368	4.458319	5.24	8.3978
$\xi_4 \times 10^{-4}$	−1.93	−1.93	−1.2815	-1.9281
λ	21.1	22.66	18.8547	21.00018
b	0.016126	0.016238	0.0136	0.016102
$R_C \times 10^{-4}$	1	2.46	7.5036	1.23
TSD	0.011819	0.011856	0.0136	0.011578

International Journal of Applied Mathematics
Volume 38 No. 12s, 2025
ISSN: 1311-1728 (printed version); ISSN: 1314-8060 (on-line version)

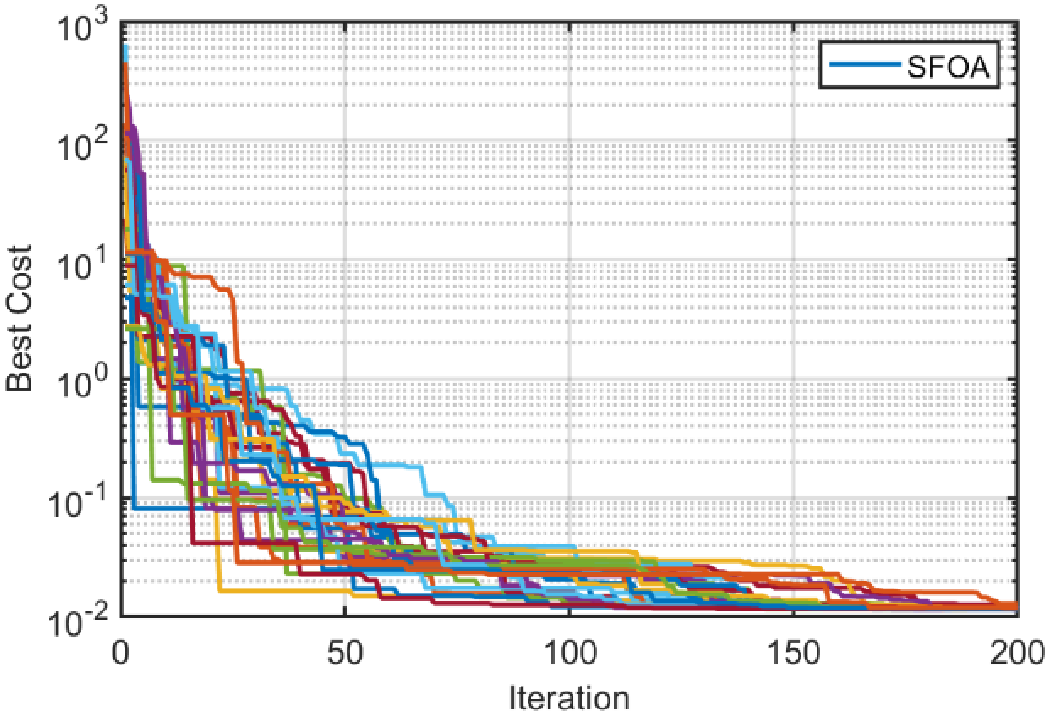

Fig. 8. Convergence curves for 30 runs for BCS 500W PEMFC using the SFOA algorithm

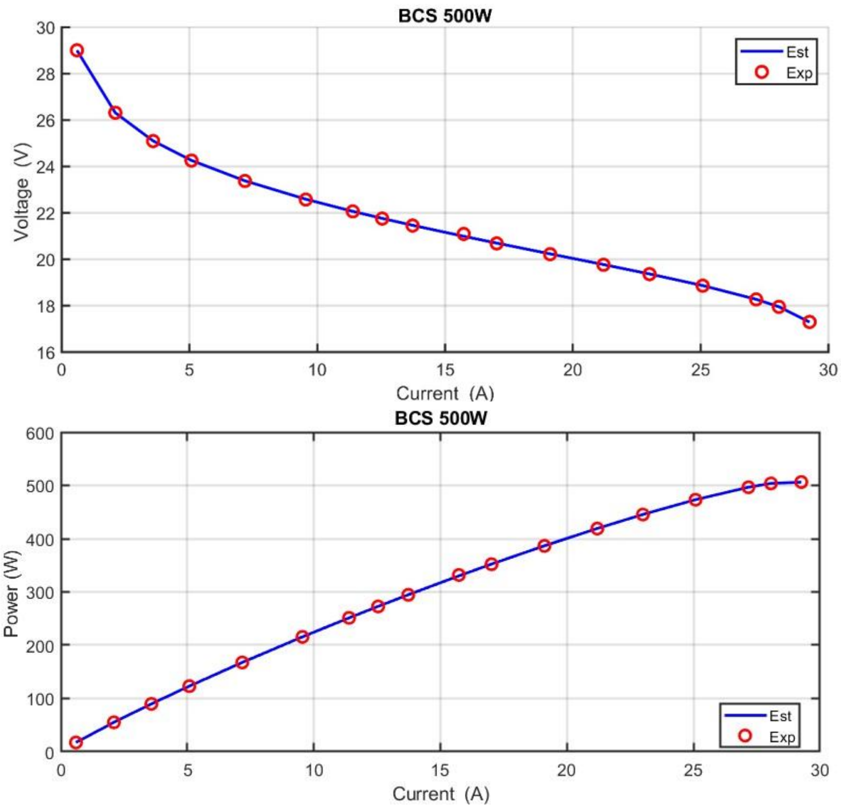

Fig. 9. Polarization curves of BCS 500W PEMFC

Received: August 14, 2025

International Journal of Applied Mathematics
Volume 38 No. 12s, 2025
ISSN: 1311-1728 (printed version); ISSN: 1314-8060 (on-line version)

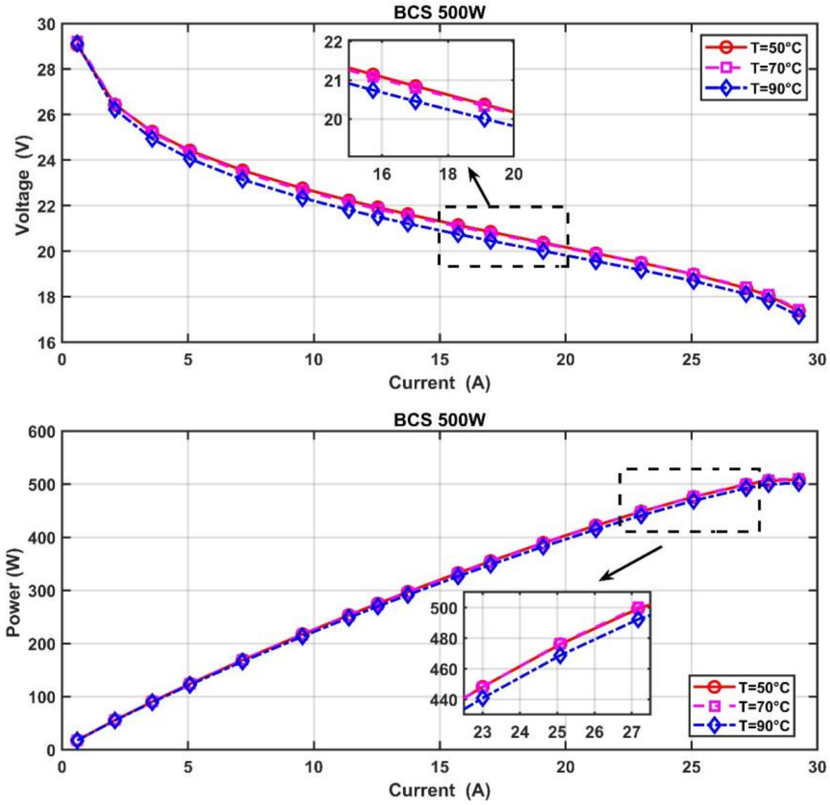

Fig. 10. Polarization curves of BCS 500W PEMFC under temperature variation.

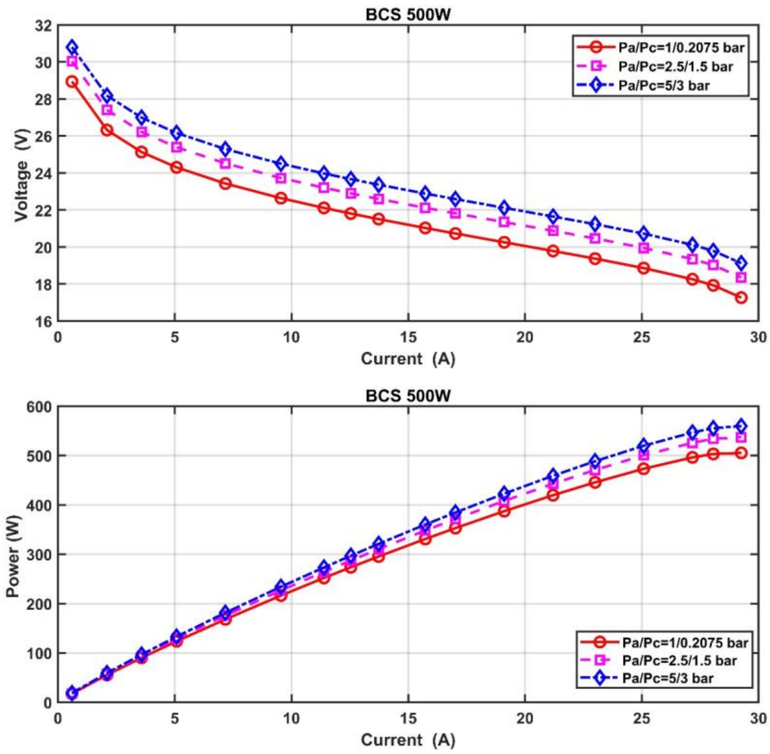

Fig. 11. Polarization curves of BCS 500W PEMFC under gases pressure variation

Received: August 14, 2025

Volume 38 No. 12s, 2025
ISSN: 1311-1728 (printed version); ISSN: 1314-8060 (on-line version)

2.3. AVISTA SR-12 PEMFC

This section analyzes SFOA on the AVISTA SR-12 PEMFC and shows it accurately recovers the model's unmeasured parameters while outperforming conventional baselines. The SFOA convergence trace (Fig. 12), exhibit fast descent and tight dispersion; Quantitatively, Table 7 reports TSD = 1.05663002 (highest accuracy for this stack) and an efficiency of 99.804%, while Table 8 shows SFOA's accuracy surpasses conventional methods (e.g., ASO at 1.0803). Polarization-curve validation built on the SFOA baseline (Fig. 13; Fig. 14; and Fig 15) demonstrates a close match between simulated and experimental I–V data and robust predictions across temperature and gas-pressure variations, confirming SFOA's reliability for AVISTA SR-12 parameter identification.

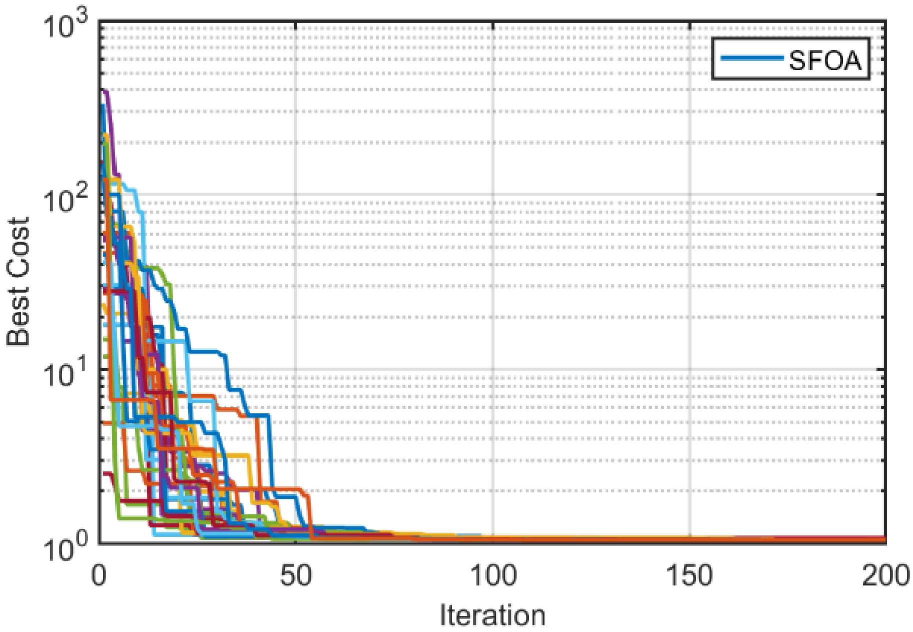

Fig. 12. Convergence curves for 30 runs for SR-12 PEMFC using SFOA algorithm

Table 7. Statistical study based on final values of convergence curves for SR-12 PEMFC.

	SFOA
Min	1.05663002
Max	1.0826195
Mean	1.058721
SD	0.0047399
MAE	0.00209098
RMSE	0.00510784
Efficiency	99.8043958

Table 8. Optimization results for SR-12 PEMFC based on the proposed methods and literature.

	SSO[37]	**ASO [35]**	**GWO [38]**	**SFOA**

ISSN: 1311-1728 (printed version); ISSN: 1314-8060 (on-line version)

ξ_1	−0.9664	−1.04314	−0.9664	-0.972148
$\xi_2 \times 10^{-3}$	2.2833	3.5928	2.2833	2.71131
$\xi_3 \times 10^{-5}$	3.40	7.70934	3.4	3.7938
$\xi_4 \times 10^{-4}$	−0.9540	−0.9540	−0.9540	-0.9540
λ	15.7969	15.9375	15.7969	23
b	0.1804	0.16905	0.1804	0.175331
$R_C \times 10^{-4}$	6.6853	7.9999	6.6853	6.7164
TSD	1.517	1.0803	1.517	1.056630

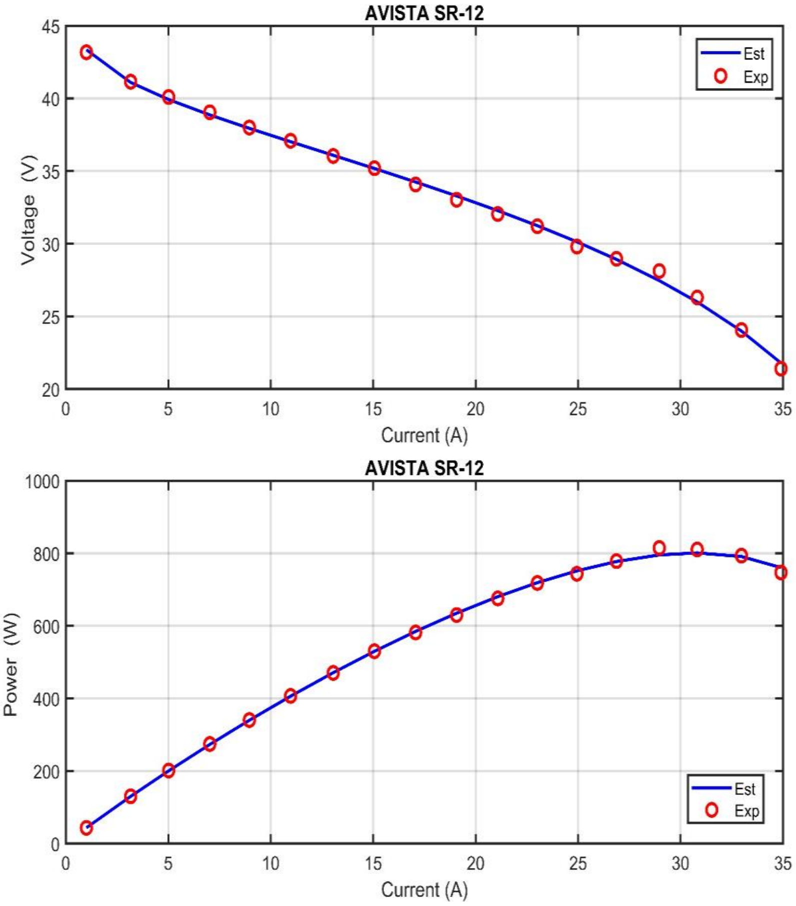

Fig. 13. Polarization curves of SR-12 PEMFC.

Received: August 14, 2025

International Journal of Applied Mathematics
Volume 38 No. 12s, 2025
ISSN: 1311-1728 (printed version); ISSN: 1314-8060 (on-line version)

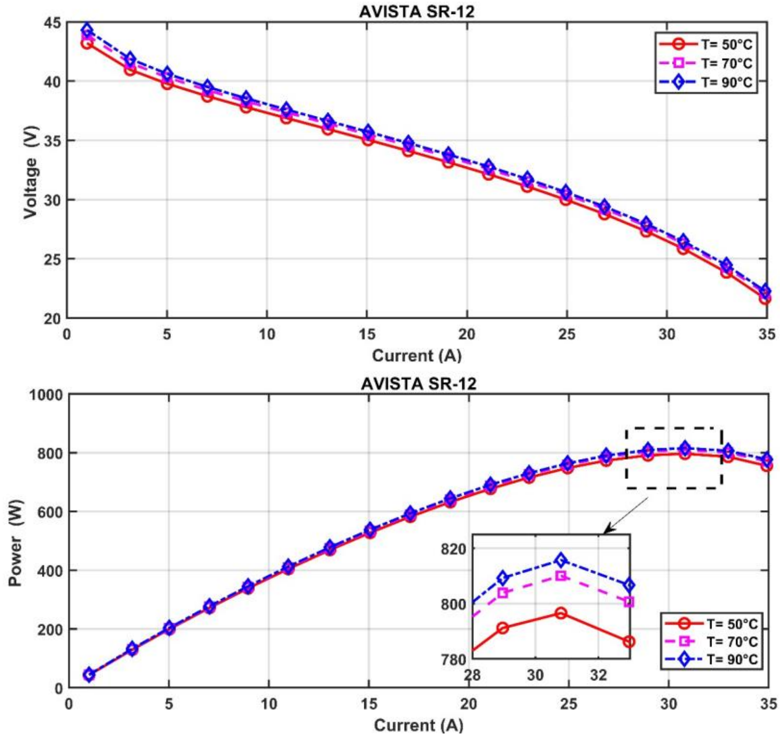

Fig. 14. Polarization curves of SR-12 PEMFC under temperature variation

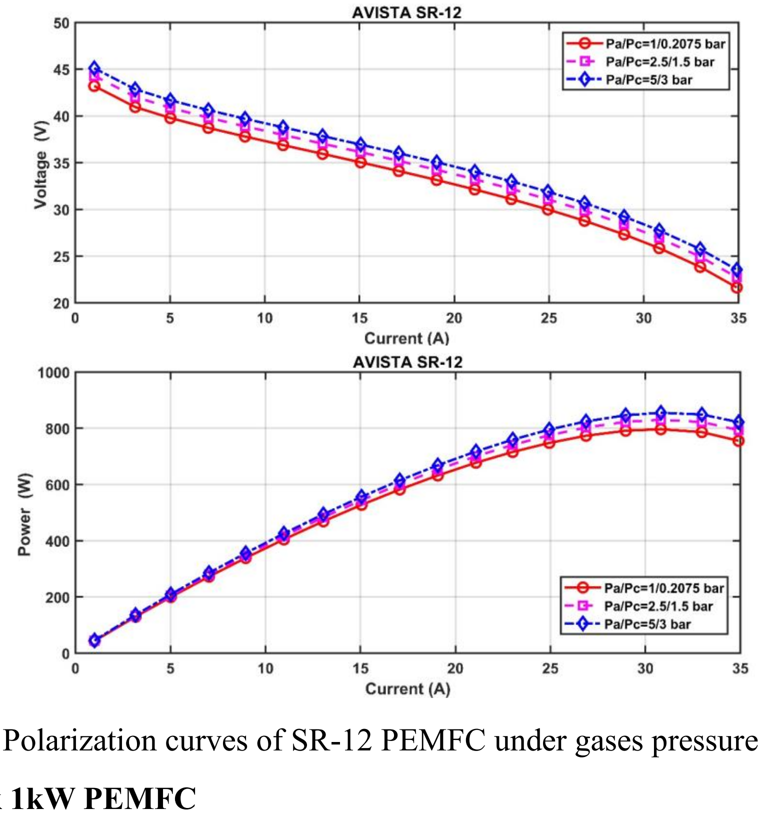

Fig. 15. Polarization curves of SR-12 PEMFC under gases pressure variation

2.4. Temasek 1kW PEMFC

Using SFOA, the Temasek 1kW PEMFC stack's unmeasured parameters are recovered with highest accuracy, achieving TSD = 0.79097446 (Table 9). The SFOA traces convergence curve (Fig. 16), Table 10 further contextualizes SFOA's accuracy against conventional baselines (SSO, SSA, GWO), where SFOA's ≈0.791 TSD improves upon the best traditional result (SSA,

Volume 38 No. 12s, 2025
ISSN: 1311-1728 (printed version); ISSN: 1314-8060 (on-line version)
≈0.793). experimental I–V data, and stress tests under varying temperature and gas pressures (Fig. 17; Fig. 18; and Fig. 19) demonstrate robust predictive performance across operating regimes.

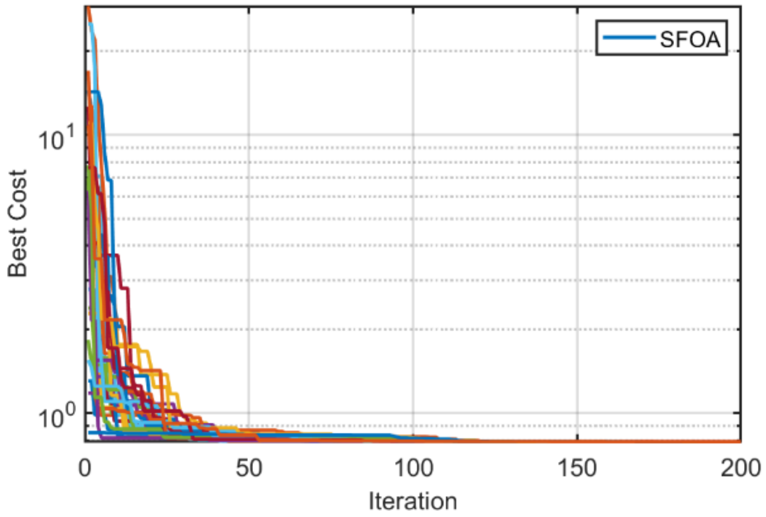

Fig. 16. Convergence curves for 30 runs for Temasek 1kW PEMFC using SFOA

Table 9. Statistical study based on final values of convergence curves for Temasek 1kW PEMFC.

	SFOA
Min	0.79097446
Max	0.79267538
Mean	0.79177511
SD	0.00050548
MAE	0.00080065
RMSE	0.00094235
Efficiency	99.8989187

Table 10. Optimization results for Temasek 1kW PEMFC based on the proposed methods and literature.

	SSO [37]	**SSA [12]**	**GWO [12]**	**SFOA**
ξ_1	−1.0299	−0.8544	−1.0299	-0.93112
$\xi_2 \times 10^{-3}$	2.4105	3.3491	2.4105	3.89181
$\xi_3 \times 10^{-5}$	4.00	6.436	4.00	8.3425
$\xi_4 \times 10^{-4}$	−9.540	−2.3417	−0.9540	-02.3014
λ	10.0005	15.309	10.001	13

$\boldsymbol{b}$	0.1274	0.077	0.1274	0.067023
$\boldsymbol{R_C \times 10^{-4}}$	1.0873	1.0094	1.0873	1.00
TSD	1.6481	0.793	1.6481	0.790974

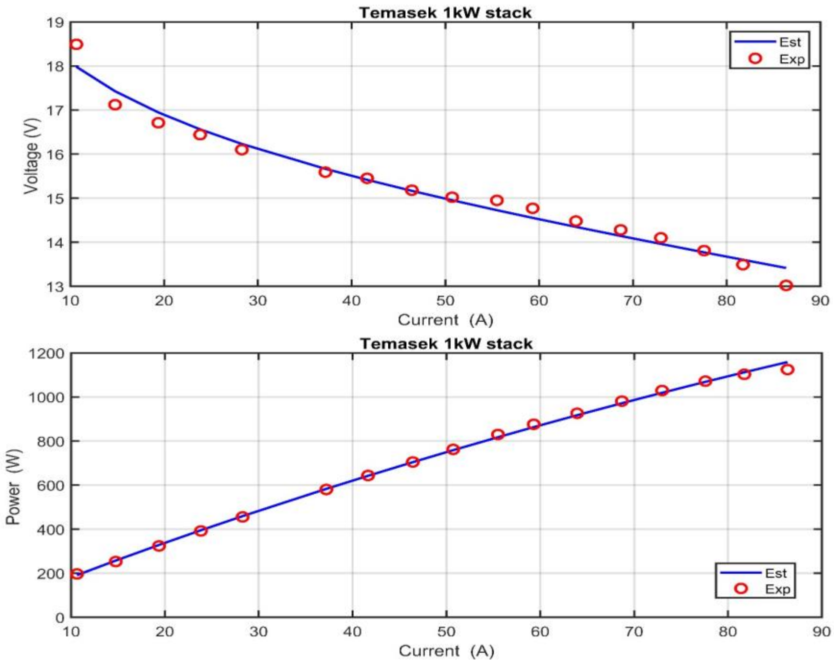

Fig. 17. Polarization curves of Temasek 1kW PEMFC

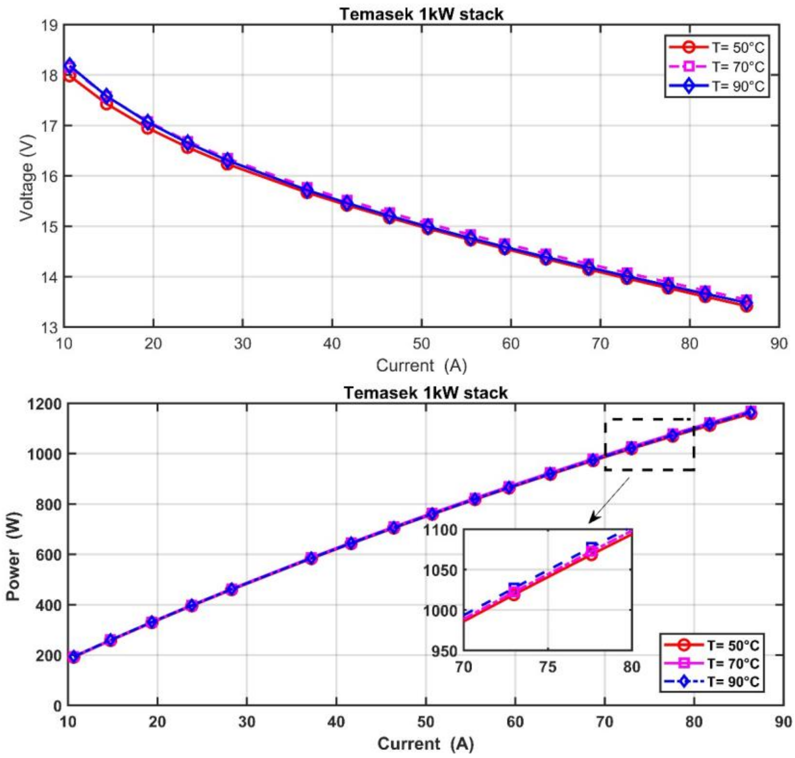

Fig. 18. Polarization curves of Temasek 1kW PEMFC under temperature variation

Received: August 14, 2025

International Journal of Applied Mathematics
Volume 38 No. 12s, 2025
ISSN: 1311-1728 (printed version); ISSN: 1314-8060 (on-line version)

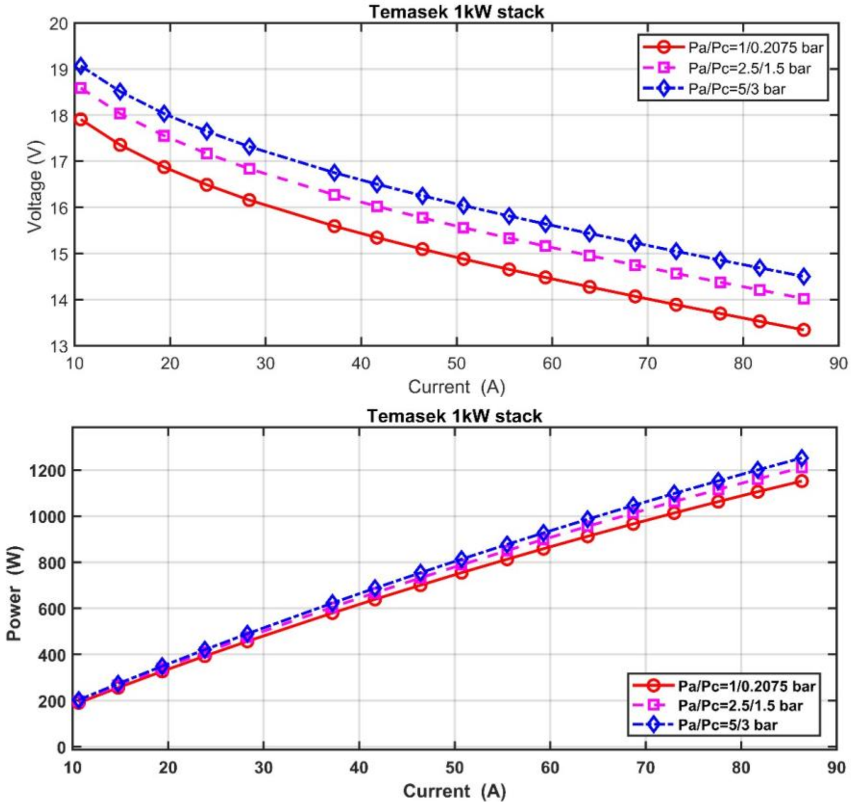

Fig. 19. Polarization curves of Temasek 1kW PEMFC under gases pressure variation.

Conclusion

This study shows that the SFOA is a reliable, accurate, and computationally efficient estimator for PEMFC semi-empirical parameters across four stacks and operating regimes (Table 11, Table 12): on the 250 W cell it achieved the lowest objective function (≈ 0.642014) with very tight dispersion (SD ≈ 5.64×10^{-4}) and near-zero error (RMSE ≈ 6.1×10^{-4}; efficiency ≈ 99.96%); for BCS-500 W, SFOA yielded efficiency ≈ 98.56%, SD ≈ 2.38×10^{-4}, and TSD ≈ 0.01158; on AVISTA SR-12, it reached TSD ≈ 1.05663 with efficiency ≈ 99.80%; and for Temasek 1 kW, it delivered the best accuracy with TSD ≈ 0.79097. Convergence plots consistently show rapid early descent and stable settling over 30 runs, while polarization-curve validation confirms close agreement with measured I–V data and correct physical trends under temperature and gas-pressure variations. With modest settings (30 agents, 200 iterations) and physically bounded search, SFOA balances exploration and exploitation effectively, generalizes across operating conditions, and provides reproducible, low-variance estimates suitable for PEMFC design, diagnostics, and control; future work can extend to dynamic/aging effects, multi-objective tuning, and online identification.

Table 11. SFOA-based parameter-estimation accuracy across four PEMFC stacks

PEMFC stack	RMSE	TSD	Efficiency (%)
250 W	0.000607079	0.642014	99.96166766
BCS-500 W	0.000291	0.01158	98.5639177

ISSN: 1311-1728 (printed version); ISSN: 1314-8060 (on-line version)

AVISTA SR-12 (500 W)	0.00510784	1.05663002	99.8043958
Temasek 1 kW	0.00094235	0.79097446	99.8989187

Table 12. Stability and experimental protocol for SFOA on the four PEMFC stacks

PEMFC stack	SD	Runs	Iter / Agents
250 W	0.000564	30	200 / 30
BCS-500 W	0.00023797	30	200 / 30
AVISTA SR-12 (500 W)	0.0047399	30	200 / 30
Temasek 1 kW	0.00050548	30	200 / 30

References

[1] T. S. Ayyarao, N. Polumahanthi, and B. Khan, "An accurate parameter estimation of PEM fuel cell using war strategy optimization," *Energy,* vol. 290, p. 130235, 2024.

[2] P. Jangir *et al.*, "A hybrid mutational Northern Goshawk and elite opposition learning artificial rabbits optimizer for PEMFC parameter estimation," *Scientific Reports,* vol. 14, no. 1, p. 28657, 2024.

[3] M. T. Özdemir, "Optimal parameter estimation of polymer electrolyte membrane fuel cells model with chaos embedded particle swarm optimization," *International Journal of Hydrogen Energy,* vol. 46, no. 30, pp. 16465-16480, 2021.

[4] Q. Niu, L. Zhang, and K. Li, "A biogeography-based optimization algorithm with mutation strategies for model parameter estimation of solar and fuel cells," *Energy conversion and management,* vol. 86, pp. 1173-1185, 2014.

[5] U. Mitra, A. Arya, and S. Gupta, "A comprehensive and comparative review on parameter estimation methods for modelling proton exchange membrane fuel cell," *Fuel,* vol. 335, p. 127080, 2023.

[6] S. Saidi *et al.*, "Precise parameter identification of a PEMFC model using a robust enhanced salp swarm algorithm," *International Journal of Hydrogen Energy,* vol. 71, pp. 937-951, 2024.

[7] A. M. Shaheen, A. Alassaf, I. Alsaleh, and A. A. El-Fergany, "Advancements in model parameter estimation for proton exchange membrane fuel cells via enhanced artificial hummingbird algorithm," *International Journal of Energy Research,* vol. 2024, no. 1, p. 7616065, 2024.

[8] H. M. Sultan, A. S. Menesy, A. Korashy, A. G. Hussien, and S. Kamel, "Enhancing parameter identification for proton exchange membrane fuel cell using modified manta ray foraging optimization," *Energy Reports,* vol. 12, pp. 1987-2013, 2024.

[9] N. Li, G. Zhou, Y. Zhou, W. Deng, and Q. Luo, "Extracting Unknown parameters of proton exchange membrane fuel cells using Quantum Encoded Pathfinder algorithm," *Frontiers in Energy Research,* vol. 10, p. 964042, 2022.

[10] J. Gupta, P. Nijhawan, and S. Ganguli, "Parameter estimation of fuel cell using chaotic mayflies optimization algorithm," *Advanced Theory and Simulations,* vol. 4, no. 12, p. 2100183, 2021.

[11] H. Rezk, A. Olabi, S. Ferahtia, and E. T. Sayed, "Accurate parameter estimation methodology applied to model proton exchange membrane fuel cell," *Energy,* vol. 255, p. 124454, 2022.

[12] H. M. Sultan, A. S. Menesy, S. Kamel, A. Selim, and F. Jurado, "Parameter identification of proton exchange membrane fuel cells using an improved salp swarm algorithm," *Energy Conversion and Management,* vol. 224, p. 113341, 2020.

[13] R. Syah *et al.*, "Developed teamwork optimizer for model parameter estimation of the proton exchange membrane fuel cell," *Energy Reports,* vol. 8, pp. 10776-10785, 2022.

[14] B. Abdollahzadeh, F. Soleimanian Gharehchopogh, and S. Mirjalili, "Artificial gorilla troops optimizer: a new nature-inspired metaheuristic algorithm for global optimization problems," *International Journal of Intelligent Systems,* vol. 36, no. 10, pp. 5887-5958, 2021.

[15] S. Mirjalili, S. M. Mirjalili, and A. Hatamlou, "Multi-verse optimizer: a nature-inspired algorithm for global optimization," *Neural computing and applications,* vol. 27, no. 2, pp. 495-513, 2016.

[16] X.-S. Yang and S. Deb, "Cuckoo search via Lévy flights," in *2009 World congress on nature & biologically inspired computing (NaBIC)*, 2009, pp. 210-214: Ieee.

[17] P. Jangir *et al.*, "A levy chaotic horizontal vertical crossover based artificial hummingbird algorithm for precise PEMFC parameter estimation," *Scientific Reports,* vol. 14, no. 1, p. 29597, 2024.

[18] M. Aljaidi *et al.*, "Artemisinin optimization: a new paradigm in computational efficiency and precision for PEMFC parameter estimation," *Ionics,* pp. 1-29, 2025.

[19] B. Ozkaya, "Optimal Parameter Estimation of PEMFC Model Using an Improved Atomic Orbital Search Algorithm," *Applications of Modelling and Simulation,* vol. 8, pp. 283-300, 2024.

[20] A. S. Menesy, H. M. Sultan, A. Korashy, S. Kamel, and F. Jurado, "A modified farmland fertility optimizer for parameters estimation of fuel cell models," *Neural Computing and Applications,* vol. 33, no. 18, pp. 12169-12190, 2021.

[21] G. Hu, Y. Guo, G. Wei, and L. Abualigah, "Genghis Khan shark optimizer: A novel nature-inspired algorithm for engineering optimization," *Advanced Engineering Informatics,* vol. 58, p. 102210, 2023.

[22] J. O. Agushaka, A. E. Ezugwu, and L. Abualigah, "Gazelle optimization algorithm: a novel nature-inspired metaheuristic optimizer," *Neural Computing and Applications,* vol. 35, no. 5, pp. 4099-4131, 2023.

[23] B. Abdollahzadeh *et al.*, "Puma optimizer (PO): a novel metaheuristic optimization algorithm and its application in machine learning," *Cluster Computing,* vol. 27, no. 4, pp. 5235-5283, 2024.

[24] C. Zhong, G. Li, Z. Meng, H. Li, A. R. Yildiz, and S. Mirjalili, "Starfish optimization algorithm (SFOA): a bio-inspired metaheuristic algorithm for global optimization compared with 100 optimizers," *Neural Computing and Applications,* vol. 37, no. 5, pp. 3641-3683, 2025.

[25] J. M. Corrêa, F. A. Farret, L. N. Canha, and M. G. Simoes, "An electrochemical-based fuel-cell model suitable for electrical engineering automation approach," *IEEE Transactions on industrial electronics,* vol. 51, no. 5, pp. 1103-1112, 2004.

[26] M. Aljaidi *et al.*, "Enhanced PEMFC Parameter Estimation Using a Hybrid Gorilla Troops Optimizer and Honey Badger Algorithm," *Computers & Chemical Engineering,* p. 109216, 2025.

[27] M. Kandidayeni, A. Macias, A. Khalatbarisoltani, L. Boulon, and S. Kelouwani, "Benchmark of proton exchange membrane fuel cell parameters extraction with metaheuristic optimization algorithms," *Energy,* vol. 183, pp. 912-925, 2019.

[28] Z. J. Mo, X. J. Zhu, L. Y. Wei, and G. Y. Cao, "Parameter optimization for a PEMFC model with a hybrid genetic algorithm," *International Journal of Energy Research,* vol. 30, no. 8, pp. 585-597, 2006.

[29] J. C. Amphlett, R. Baumert, R. F. Mann, B. A. Peppley, P. R. Roberge, and T. J. Harris, "Performance modeling of the Ballard Mark IV solid polymer electrolyte fuel cell: II. Empirical model development," *Journal of the Electrochemical Society,* vol. 142, no. 1, p. 9, 1995.

[30] B. Chakraborty, A. Bera, D. Muthu, S. Bhowmick, U. V. Waghmare, and A. Sood, "Symmetry-dependent phonon renormalization in monolayer MoS 2 transistor," *Physical Review B—Condensed Matter and Materials Physics,* vol. 85, no. 16, p. 161403, 2012.

[31] J. Thepkaew, A. Therdthianwong, and S. Therdthianwong, "Key parameters of active layers affecting proton exchange membrane (PEM) fuel cell performance," *Energy,* vol. 33, no. 12, pp. 1794-1800, 2008.

[32] H. Rezk *et al.*, "Optimal parameter estimation strategy of PEM fuel cell using gradient-based optimizer," *Energy,* vol. 239, p. 122096, 2022.

[33] A. Sohani, S. Naderi, and F. Torabi, "Comprehensive comparative evaluation of different possible optimization scenarios for a polymer electrolyte membrane fuel cell," *Energy Conversion and Management,* vol. 191, pp. 247-260, 2019.

Volume 38 No. 12s, 2025
ISSN: 1311-1728 (printed version); ISSN: 1314-8060 (on-line version)
[34] J. Cheng and G. Zhang, "Parameter fitting of PEMFC models based on adaptive differential evolution," *International Journal of Electrical Power & Energy Systems,* vol. 62, pp. 189-198, 2014.

[35] M. A. Mossa, O. M. Kamel, H. M. Sultan, and A. A. Z. Diab, "Parameter estimation of PEMFC model based on Harris Hawks' optimization and atom search optimization algorithms," *Neural Computing and Applications,* vol. 33, no. 11, pp. 5555-5570, 2021.

[36] S. Xu, Y. Wang, and Z. Wang, "Parameter estimation of proton exchange membrane fuel cells using eagle strategy based on JAYA algorithm and Nelder-Mead simplex method," *Energy,* vol. 173, pp. 457-467, 2019.

[37] Y. Rao, Z. Shao, A. H. Ahangarnejad, E. Gholamalizadeh, and B. Sobhani, "Shark Smell Optimizer applied to identify the optimal parameters of the proton exchange membrane fuel cell model," *Energy conversion and management,* vol. 182, pp. 1-8, 2019.

[38] M. Ali, M. El-Hameed, and M. Farahat, "Effective parameters' identification for polymer electrolyte membrane fuel cell models using grey wolf optimizer," *Renewable energy,* vol. 111, pp. 455-462, 2017.

Received: August 14, 2025